Letter

Evolutionary dynamics in a varying environment: Continuous versus discrete noise

Ami Taitelbaum,[1] Robert West [ID],[2] Mauro Mobilia [ID],[2,*] and Michael Assaf [ID][1,3,†]

[1]*Racah Institute of Physics, Hebrew University of Jerusalem, Jerusalem 91904, Israel*
[2]*Department of Applied Mathematics, School of Mathematics, University of Leeds, Leeds LS2 9JT, United Kingdom*
[3]*Institute of Physics and Astronomy, University of Potsdam, Potsdam 14476, Germany*

Environmental variations can significantly influence how populations compete for resources, and hence shape their evolution. Here, we study population dynamics subject to a fluctuating environment modeled by a varying carrying capacity changing continuously in time according to either binary random switches, or by being driven by a noise of continuous range. We focus on a prototypical example of two competing strains, one growing slightly slower than the other. By systematically comparing the effect of a binary versus continuously varying environment, we study how different noise statistics (mean, variance) influence the population size and fixation properties. We show that the slow strain fixation probability can be greatly enhanced for a continuously varying environment compared to binary switches, even when the first two moments of the carrying capacity coincide.

Natural populations face endlessly varying environmental conditions, such as the abundance of nutrients or toxins, temperature, light, and humidity, all of which influence their interactions and evolution [1–3]. In the absence of detailed knowledge of how external factors change, they are often modeled as environmental noise (EN). This in turn shapes the fluctuating environment where populations evolve, for which several response mechanisms have been proposed [4–27]. Apart from EN, demographic noise (DN) is another source of randomness: It can lead to fixation, when one species takes over the population, and its effect is significant in small communities, but negligible in large populations [28–31].

Importantly, the evolution of the size and composition of a multispecies population are often interdependent [32–40]. This may result in a coupling between DN and EN, with external factors affecting the population size, which in turn modulates the DN intensity. The interplay between EN and DN is crucial in microbial communities, which can experience sudden, extreme environmental changes [41–48], as well as in ecology [15–17]. In the context of antimicrobial resistance, variations of population size and composition are key when antibiotics reduce a large community to a very small size, but fail to eradicate it. Surviving cells in the small population, prone to fluctuations, may then replicate and restore infections, with survivors likely to develop antibiotic resis-

tance [27,43]. Interactions between microbial communities and the environment can also lead to population bottlenecks, where new colonies of few individuals result in cooperative behavior [45–47]. In most theoretical studies involving multiple species, there is no explicit interdependence between EN and DN. Growth rates are thus commonly assumed to be subject to noise of continuous range [6,7,21–23,49], and vary independently of the population size that is often constant [11–14,18,19,22,23,25,50–57]. On the other hand, there have been numerous laboratory-controlled experiments with microbial communities of varying sizes evolving by switching instantaneously between a *discrete* number of environmental states ("discrete EN"), with a strong focus on the binary case [11,40,42,46,48,57,58]. This has motivated the study of population models with random binary switching of the species growth rates [5,11,17,52,54,55], and more recently of the carrying capacity (or resources) leading to the coupling of DN and EN [32,33,59–61].

Nevertheless, *in vivo* exogenous factors often vary continuously, in time and over a range of values [62,63], rather than by instantaneous switches. For instance, the carrying capacity of certain phytoplankton species and the growth rates of some algae vary with fluctuating temperature [64–66]. It is thus important to understand how the coupling of DN and EN affects the dynamics of communities in an environment varying along a continuum of states ("continuous EN"), and to compare its properties with those in binary fluctuating environments commonly used in experiments [11,40,42,46,48,57,58] and theory [5,17,32,33,52,54,55,60,61].

Here, we address these questions by systematically investigating the influence of coupled DN and EN on the evolution of a simplified microbial community consisting of two competing strains, one growing slightly slower than the other, subject to a carrying capacity driven either by binary or continuous EN. For this simplified microbial model, we unveil the similarities and differences of evolving under continuous

---

*Author to whom correspondence should be addressed: m.mobilia@leeds.ac.uk

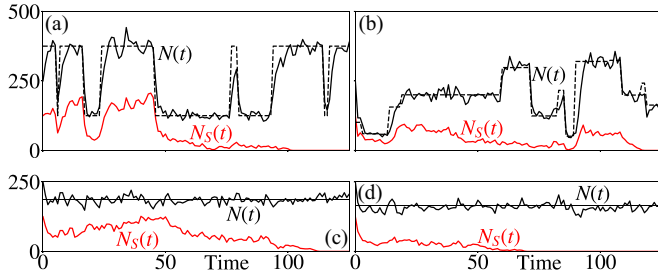†Author to whom correspondence should be addressed: michael.assaf@mail.huji.ac.il

FIG. 1. Typical realizations of N (black) and N_S (red/gray) vs time under symmetric EN of variance σ^2: binary D-noise in (a) and (c), and continuous U-noise in (b) and (d). (a), (b) $\nu = 0.1$, where dashed lines show $K(t)$. (c), (d) $\nu = 1000$, where solid horizontal lines show (c) $\mathcal{K}_D$ and (d) $\mathcal{K}_U$, given by Eq. (8), about which N fluctuates under high ν (see text). In all panels $(s, x_0, K_0, \sigma) = (0.02, 0.5, 250, 0.5)$, and $N(0) = K_0$.

or binary EN, and reveal the drastic effect that EN may have on the population size distribution and fixation properties. Remarkably, we show that the slow species fixation probability can be significantly enhanced under continuous noise over its value under binary EN of same mean and variance. The generalization to a scenario of cooperative behavior is briefly discussed in the Supplemental Material (SM) [67].

We consider a well-mixed population consisting of N_S individuals of a slow-growing strain S and N_F microbes of the fast-growing strain F. At time t, this two-strain population has a time-fluctuating size $N(t) = N_S(t) + N_F(t)$ and is composed of a fraction $x = N_S/N$ of slow growers S. Per-capita growth rates are $(1 - s)/\bar{f}$ for S and $1/\bar{f}$ for F, where $\bar{f} = 1 - sx$ is the population average fitness, and $0 < s \ll 1$ denotes the small growth advantage (selective bias) of F over S [32,33,35,36,59]. Owing to limited and varying resources, the strain's growth is limited by a logistic death rate $N/K_\ell(t)$, where $K_\ell(t) \gg 1$ is the carrying capacity that here fluctuates in time due to EN. This allows us to couple in a simple and biologically relevant way DN and EN [32,33,59–61], which yields the following birth-death process [33,68],

$$N_{S/F} \xrightarrow{T_{S/F}^+} N_{S/F} + 1 \quad \text{and} \quad N_{S/F} \xrightarrow{T_{S/F}^-} N_{S/F} - 1, \quad (1)$$

with transition rates $T_S^+ = (1 - s)N_S/\bar{f}$, $T_F^+ = N_F/\bar{f}$, and $T_{S/F}^- = (N/K_\ell)N_{S/F}$. We model EN by letting the carrying capacity fluctuate in time as

$$K_\ell(t) = K_{0,\ell}[1 + \xi_\ell(t)], \quad (2)$$

where $\xi_\ell(t)$ denotes the stationary symmetric EN of type $\ell \in \mathcal{L} \equiv \{D, U, B\}$, with discrete or continuous range. For the former, we focus on the *symmetric dichotomous* ($\ell = D$, or *telegraph*) noise [69,70], and for the latter we consider EN with uniform ($\ell = U$) and symmetric beta ($\ell = B$) stationary probability density function (PDF) $p^*(\xi_\ell)$ of support $\mathcal{S}_\ell$ [67]. It is convenient to denote the set of EN with continuous range (continuous EN) as $\ell \in \mathcal{L}' \equiv \mathcal{L} \setminus D$.

For $\ell = D$, the random process $\xi_D \to -\xi_D$, where $\xi_D \in \{-\sigma_D, \sigma_D\}$ ($0 < \sigma_D < 1$), occurs at a rate $\nu/2$ and has a correlation time $1/\nu$. Hence, K_ℓ switches between a high and low value after an average time $2/\nu$ (see Fig. 1).

For $\ell \in \mathcal{L}'$, ξ_ℓ is a colored continuous EN with correlation time $1/\nu$ defined by the stochastic differential equation, in the sense of Itô calculus [67,68],

$$d\xi_\ell = -\nu\xi_\ell dt + \sqrt{\mathcal{B}_\ell}\, dW, \quad (3)$$

where $W \sim \mathcal{N}(0, 1)$ is the normally distributed Wiener process of zero mean and unit variance. The first term on the right-hand side of (3) represents the linear drift, and the second is the diffusion term. For concreteness and simplicity, we focus on symmetric continuous EN: $\ell = B$ (beta) and $\ell = U$ (uniform) as examples of EN for which K_ℓ has a zero and finite lower bound, respectively. In the former, ξ_B is distributed according to a single-parameter ($\beta > 1$) symmetric beta distribution on $(-1, 1)$, with variance $\sigma_B^2 = 1/(2\beta + 1) < 1/3$; in the latter ξ_U is uniformly distributed on $(-\sigma_U\sqrt{3}, \sigma_U\sqrt{3})$ with variance $\sigma_U^2 < 1/3$ (see Fig. 1). The diffusive terms satisfy [67]

$$\mathcal{B}_U = \nu(3\sigma_U^2 - \xi_U^2), \quad \mathcal{B}_B = \nu\left(\frac{2\sigma_B^2}{1 - \sigma_B^2}\right)(1 - \xi_B^2). \quad (4)$$

Notably, the coupling of (1)–(3) generally yields a *non-Markovian* process (when $\nu \neq 0$) (see Sec. A2 of SM [67]).

The PDF of K_ℓ, $\mathcal{P}(K_\ell)$, can be obtained from $p^*(\xi_\ell)$ and Eq. (2) [67]. Below we focus on the first two moments of K_ℓ (skewness vanishes for symmetric EN). To meaningfully compare the influence of discrete and continuous EN on population dynamics, we impose the same first two moments, yielding $K_{0,D} = K_{0,\ell} = K_0$ and $\sigma^2 = \sigma_D^2 = \sigma_\ell^2$ for $\ell \in \mathcal{L}'$, as long as $\sigma_\ell^2 < \sigma_{max}^2 \equiv 1/3$ [67]. Henceforth, as long as $\sigma_\ell < \sigma_{max}$ we denote σ_ℓ by σ for all forms of EN.

Ignoring fluctuations, in the limit of an infinite population with constant carrying capacity $K(t) = K_0 \gg 1$, the resulting mean-field dynamics yields $\dot{N} = N(1 - N/K_0)$ and $\dot{x} \approx -sx(1 - x)$ [32,33,35,59]. This indicates a timescale separation between the typical relaxation time of N, $t = O(1)$, and that of x, $t \sim 1/s \gg 1$. Accounting for DN, the above timescales represent the convergence of the population size distribution (PSD) to the long-lived metastable state centered about K_0, after $t = O(1)$, and the fixation of one of the species (and extinction of the other), at $t \sim 1/s$ [32,33,67,71].

Indeed, in a finite population, random birth/death events lead to the fixation of one strain. The slow-grower fixation probability in a population of constant size N, given an initial $x_0 = N_S(0)/N(0)$, satisfies $\phi(N, s, x_0) = (e^{-Nx_0 \ln(1-s)} - 1)/(e^{-N \ln(1-s)} - 1) \approx e^{N(1-x_0)\ln(1-s)}$, where the approximation holds when $-N\ln(1 - s) \gg 1$ [29,72], and when N fluctuates about $K_0 \gg 1$ [32,33,59]. However, the fixation probability changes dramatically when K_ℓ varies according to (2). Since EN varies either discretely or continuously, we characterize the population dynamics by studying the joint influence of EN and DN on the fixation properties and PSD as function of ν and σ.

In the case of D-EN, the full PSD, $P_\ell(N, \nu)$, can be well approximated in all regimes by the PDF of a piecewise-deterministic Markov process associated with (1) and (2) [32,33,59–61,67,73]. Yet, there is no equivalent method to approximate the PSD for all ν under continuous EN, and $P_\ell(N, \nu)$ is thus obtained numerically (see Sec. A3 and Fig. S1 in SM [67]). As detailed below, analytical

progress is however possible in the regime $\nu \ll s$ (long correlation time), when $K_\ell(t) \approx K_\ell(0)$ and $P_\ell(N, \nu/s) \approx \mathcal{P}(K_\ell)$, and when $\nu \gg s$ (short correlation time). In the latter regime, $P_\ell(N, \nu/s) \approx \delta(N - \mathcal{K}_\ell)$ [see Eqs. (7) and (8) and Fig. S1(c) in SM [67]]. Furthermore, when $\nu \gg s$ and $\sigma \ll 1$, $P_\ell(N, \nu)$ can be computed more accurately within a WKB approximation (see Sec. A2.3 in SM [67]). Once the PSD is found, numerically or analytically, we can use the timescale separation to find the S-fixation probability under ℓ-EN, ϕ_ℓ. In fact, as the population settles in its long-lived PSD after $t = O(1)$, i.e., much earlier than fixation that occurs after $t = O(1/s) \gg 1$ (with a weak N dependence) [30,32,33], and given x_0, ϕ_ℓ can be found by averaging $\phi(N, s, x_0)$ over $P_\ell(N, \nu/s)$:

$$\phi_\ell \simeq \int_0^\infty P_\ell(N, \nu/s)\phi(N, s, x_0)dN. \qquad (5)$$

Here, we have rescaled $\nu \to \nu/s$ corresponding to $O(\nu/s)$ environmental switches that the population experiences prior to fixation [32,33,59]. This result holds under weak selection, $1/K_0 \ll s \ll 1$. A similar approach allows us to obtain the mean fixation time $T_\ell = O(1/s)$ (see Sec. A4 in SM [67]). Before considering the general case using (5), we now study the PSD and ϕ_ℓ in the regimes of long- and short-correlated EN.

Low varying rate (long-correlated EN). When $\nu \ll s$, the environment barely changes prior to fixation of either species (after $t \sim 1/s$), and is assumed to be stationary as N rapidly equilibrates, with $P_\ell(N) \approx \mathcal{P}(K_\ell)$ (see Sec. A2 in SM [67]). We thus approximate ϕ_ℓ by $\phi_\ell^0 = \int \mathcal{P}(K_\ell)\phi(K_\ell, s, x_0)dK_\ell$ [67]. Here, the PSD is unimodal (or flat) under continuous EN, in sharp contrast to the bimodal PSD obtained for D-EN [32] [see Figs. S1(a) and S1(b) in SM [67]]. When $K_0 s \gg 1$ and $s \ll 1$, we have $\phi(N, s, x_0) \approx \exp(-\eta N)$ with $\eta \equiv -(1 - x_0)\ln(1 - s) \simeq s(1 - x_0) > 0$. By integrating over $\mathcal{P}(K_\ell)$, we find

$$\phi_\ell^0 = \begin{cases} e^{-\eta K_0}\cosh(\eta K_0 \sigma) & \text{(D)}, \\ \int_{-1}^1 e^{-\eta K_0(1+\xi)}\frac{(1+\xi)^{\beta-1}(1-\xi)^{\beta-1}}{B(\beta,\beta)2^{2\beta-1}}d\xi & \text{(B)}, \\ \frac{e^{-\eta K_0}}{\eta K_0 \sigma\sqrt{3}}\sinh(\eta K_0 \sigma\sqrt{3}) & \text{(U)}, \end{cases} \qquad (6)$$

where $\beta \equiv (1 - \sigma^2)/(2\sigma^2)$ and $B(\beta, \beta) \equiv \int_0^1 t^{\beta-1}(1 - t)^{(\beta-1)}dt$ is the beta function. In Fig. 2(a) we show the dependence of ϕ_ℓ^0 on σ when K_0 is kept fixed, which agrees well with simulation results. We find that EN can enhance the S-fixation probability by several orders of magnitude with respect to $\phi(K_0, s, x_0)$, its static-environment counterpart [32,33,67] (see Fig. S3 of SM [67]). Moreover, $\phi_{\ell \in \mathcal{L}'}^0$ under continuous EN is much larger than ϕ_D^0. This stems from $P_{\ell \in \mathcal{L}'}$ having a broad left tail enhancing ϕ_ℓ^0 compared to the contribution arising from the left peak of P_D [see Eq. (5) and Figs. S1(a) and S1(b) in SM [67]].

High varying rate (short-correlated EN). When $\nu \gg s$ and $K_0 \gg 1$ (with σ not too close to $\sigma_{\max}$), ϕ_ℓ is governed by EN that dominates over DN [59,67]. In fact, under high ν,

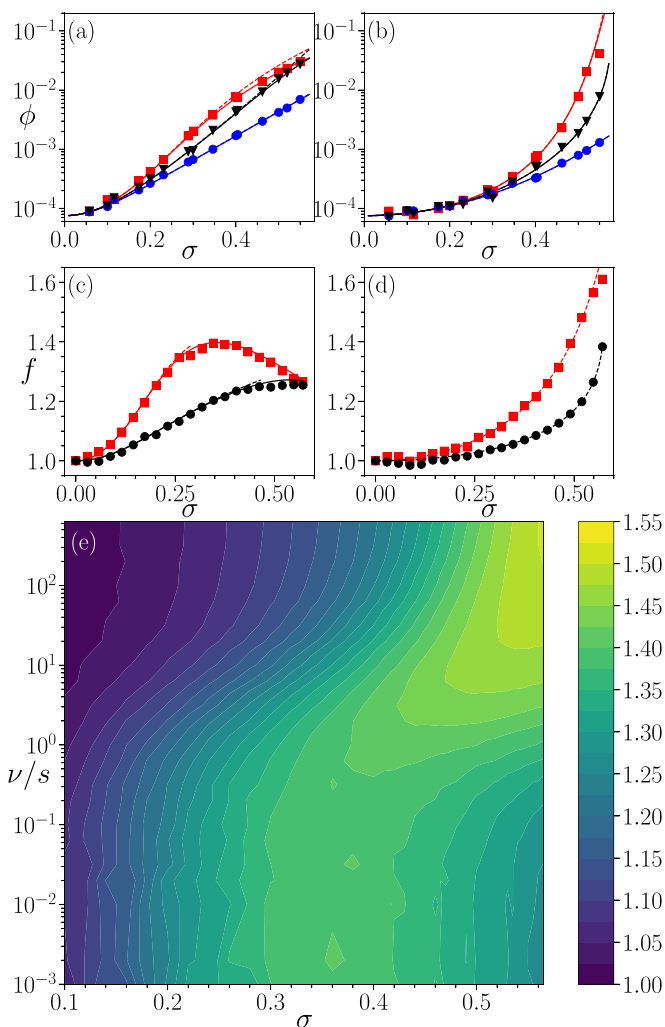
FIG. 2. (a) ϕ_ℓ^0 vs σ and (b) ϕ_ℓ^∞ vs σ under symmetric ℓ-EN. (c) f_ℓ^0 vs σ and (d) f_ℓ^∞ vs σ, where f_ℓ is the standard-deviation multiplier obtained by solving $\phi_D^{(0,\infty)}(f_\ell^{(0,\infty)}\sigma) = \phi_{\ell \in \mathcal{L}'}^{(0,\infty)}(\sigma)$ with K_0 kept fixed (see text). Symbols in (a) and (b) are from simulations, and in (c) and (d) are from a numerical evaluation of (5) using simulation histograms for P_ℓ. Dashed lines are from Eqs. (6) in (a) and (c) and (8) in (b) and (d), while solid lines in (a)–(c) are from a numerical evaluation of (5) using analytical results for P_ℓ in the low/high ν limit. In (a)–(d), blue/dark gray stands for $\ell = D$, black for $\ell = U$, and red/gray for $\ell = B$. Simulation results for ϕ_ℓ^0 and ϕ_ℓ^∞ were obtained for $\nu = 10^{-4}$ and $\nu = 3 \times 10^3$, respectively. (e) Heat map of the multiplier f_B vs σ and ν (see text). Dark areas interspersed by lighter regions indicate where $f_B(\sigma)$ is nonmonotonic (slow/intermediate ν regimes). In all panels $(K_0, s, x_0) = (750, 0.025, 0.5)$, and $\sigma < \sigma_{\max}$ for proper comparison of the different EN. A similar heat map is obtained for U-EN, with the main qualitative difference being the absence of nonmonotonicity.

N obeys the logistic stochastic differential equation $\dot{N} = N[1 - N/K(t)]$, with the environment varying so frequently that EN self-averages, yielding $\dot{N} = N(1 - N/\mathcal{K}_\ell)$ [32,33,59], where [67]

$$\mathcal{K}_\ell \equiv \frac{K_0}{\left\langle \frac{1}{1+\xi_\ell} \right\rangle} \equiv K_0 \left[\int_{\mathcal{S}_\ell} \frac{p^*(\xi_\ell)}{1 + \xi_\ell}d\xi_\ell \right]^{-1}. \qquad (7)$$

For symmetric ℓ-EN, we explicitly find

$$\frac{\mathcal{K}_D}{K_0} = 1 - \sigma^2, \quad \frac{\mathcal{K}_B}{K_0} = 1 - \frac{\sigma^2}{1 - 2\sigma^2},$$

$$\frac{\mathcal{K}_U}{K_0} = \frac{\sqrt{3}\sigma}{\tanh^{-1}(\sqrt{3}\sigma)}. \tag{8}$$

This dependence yields $\mathcal{K}_B < \mathcal{K}_U < \mathcal{K}_D$ for fixed σ [see Fig. S2(a) of SM [67]]. $P_\ell(N, \nu/s)$ is very narrow and centered around $\mathcal{K}_\ell$ when $\nu \gg s$ [see Fig. S1(c) of SM [67]]. Hence, upon ignoring DN, Eq. (5) can be crudely approximated using $P_\ell(N, \nu/s) \approx \delta(N - \mathcal{K}_\ell)$, yielding $\phi_\ell \to \phi_\ell^\infty \approx \exp(-\eta\mathcal{K}_\ell)$: When $\nu/s \gg 1$, high environmental variability ensures self-averaging prior to fixation, leading to $\phi_\ell \approx \phi_\ell^\infty$. According to (8) the values of $\mathcal{K}_\ell$ for $\ell \in \mathcal{L}'$ are markedly lower than $\mathcal{K}_D$, especially when σ approaches $\sigma_{\max}$. This implies $\phi_{\ell \in \mathcal{L}'}^\infty \gg \phi_D^\infty$, as confirmed by Fig. 2(b), whose predictions agree well with simulation data. Also, ϕ_ℓ^∞ is generally significantly larger than its static-environment counterpart (see Fig. S3 of SM [67]).

Intermediate varying rate (general case). When $\nu \sim s$, we compute ϕ_ℓ using (5). While an analytical approximation can be obtained under D-EN [32,33,59,61], Eq. (5) is evaluated numerically under continuous EN by integrating over the PSD obtained from simulation data. We find that Eq. (5) provides an accurate approximation of ϕ_ℓ over a broad range of ν/s for all forms of ℓ-EN (see Fig. S3 of SM [67]). This approximation agrees well with ϕ_ℓ^0 when $\nu/s \ll 1$ and ϕ_ℓ^∞ when $\nu/s \gg 1$ [67].

Most laboratory-controlled experiments on fluctuating populations are carried out by probing a discrete set (often binary) of environmental states [11,56–58,74]. Yet, many *in vivo* exogenous factors can take a continuous range of values, and little is known on the joint effects of continuously varying environmental conditions and DN. We thus analyze the effects of discrete and continuous EN on population dynamics, by systematically comparing ϕ_D under D-noise with $\phi_{B/U}$ under B/U-EN. Keeping K_0 and σ fixed for every ℓ-EN, we have determined the multiplier f_ℓ by which the variance of the D-noise needs to be enhanced ($\sigma \to f_\ell\sigma$) for ϕ_D to match $\phi_{\ell \in \mathcal{L}'}$, for given ν. In practice, we have generally used (5) to determine f_ℓ by numerically solving $\phi_D(f_\ell\sigma) = \phi_\ell(\sigma)$ over $\sigma \in (0, \sigma_{\max})$ for $\ell \in \mathcal{L}'$ and fixed ν (see Sec. A3 in SM [67]). As shown in Figs. 2(c)–2(e), f_ℓ is a nontrivial function of ν and σ, with $f_\ell \geqslant 1$ reflecting the fact that a higher variance of D-EN is necessary to achieve the same fixation probability as under B/U-EN. For long- and short-correlated EN ($\nu/s \ll 1$ and $\nu/s \gg 1$, respectively) we have used (6) and (8) to determine the multipliers f_ℓ^0 and f_ℓ^∞ analytically. These predictions, shown in Figs. 2(c) and 2(d), agree well with simulation results. For $\sigma \ll 1$, in the limit $\nu \to 0$, one has $f_U^0 \approx 1 + (\eta K_0\sigma)^2/30$, $f_B^0 \approx 1 + (\eta K_0\sigma)^2/12$, while $f_U^\infty \approx 1 + (2/5)\sigma^2$ and $f_B^\infty \approx 1 + \sigma^2$ when $\nu \gg s$. Remarkably, f_B exhibits a nonmonotonic dependence on σ when $\nu/s \ll 1$ and $\nu/s \sim 1$ [see Figs. 2(c) and 2(e)]: The multiplier $f_B(\sigma)$ attains a maximum at σ_f ($0 < \sigma_f < \sigma_{\max}$), while the maximum of f_U occurs at $\sigma_f \approx \sigma_{\max}$. Hence, the leveling (stabilizing) effect of B-EN on the competition compared to D-EN in the slow/intermediate regimes is maximal for $\sigma \approx \sigma_f$. Con-
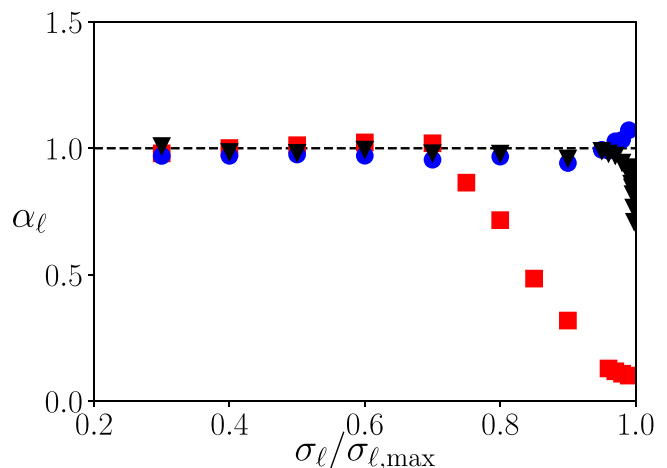

FIG. 3. Exponent α_ℓ of (9) vs $\sigma_\ell/\sigma_{\ell,\max}$ in the regime $\nu/s \gg 1$. Here, $\sigma_{\ell,\max} = 1/\sqrt{3}$ for $\ell \in \mathcal{L}'$ and $\sigma_{\ell,\max} = 1$ for D-EN. Red squares, blue circles, and black triangles correspond to (B,D,U)-EN, respectively, and the dashed line is a guide to the eye showing $\alpha_\ell = 1$. Here, $(K_0, s, x_0) = (900, 0.025, 0.5)$, and different values of $\nu \gg s$, with $\nu \in [12s, 4000s]$ [67].

versely, f_ℓ increases with σ when $\nu/s \gg 1$ [see Figs. 2(d) and 2(e)].

Having shown that continuous EN can drastically enhance the fixation probability compared to binary EN, we have also studied how ϕ_ℓ^∞ is approached when $\nu/s \gg 1$. As ν increases, we find that ϕ_ℓ converges towards ϕ_ℓ^∞ according to the following scaling, illustrated in Fig. 3,

$$\phi_\ell(\nu) \simeq \phi_\ell^\infty \exp\left[\mathcal{A}_\ell(s/\nu)^{\alpha_\ell}\right], \tag{9}$$

where the parameter $\mathcal{A}_\ell$ depends on K_0, η and σ. In the case of D-EN, we found $\alpha_D \approx 1$ regardless of σ [59]. In the case of continuous EN, $\alpha_{\ell \in \mathcal{L}'} \approx 1$ for small σ (see Sec. A2.3 in SM [67]), yet $\alpha_{\ell \in \mathcal{L}'}$ decreases as $\sigma \to \sigma_{\max}$, indicating a slower convergence to ϕ_ℓ^∞ with B/U-EN than under D-EN. As shown in Fig. 3, the convergence is particularly slow under B-EN when $\sigma_B \approx \sigma_{\max} = 1/\sqrt{3}$, while the effect is weaker under U-EN. This stems from $\mathcal{K}_\ell$ attaining low values with nonzero probability under continuous EN, yielding a slower convergence of the average value of N to $\mathcal{K}_\ell$ than under D-EN (see Sec. A.2.2 in SM [67]).

We have studied the competition for resources of two strains subject to DN coupled to either binary or continuously varying EN. Our findings suggest that population dynamics is drastically affected by the form of EN: Continuous EN generally *levels the field of competition* and significantly increases the fixation probability of the slower strain S. This finding is rationalized by mapping results of continuous EN onto those from binary EN (see Fig. 2). Furthermore, the analysis can be generalized to describe the ecoevolutionary dynamics of cooperative behavior [67]. Our results, demonstrating that discrete and continuous EN, jointly with DN, can have markedly different effects on how populations compete for resources, pave the way to a better understanding of the influence of such environmental conditions on the evolution of *in vivo* microbial communities.

[1] C. R. Morley, J. A. Trofymow, D. C. Coleman, and C. Cambardella, Effects of freeze-thaw stress on bacterial populations in soil microcosms, Microbiol. Ecol. **9**, 329 (1983).

[2] C. A. Fux, J. W. Costerton, P. S. Stewart, and P. Stoodley, Survival strategies of infectious biofilms, Trends Microbiol. **13**, 34 (2005).

[3] J. G. Caporaso, C. L. Lauber, E. K. Costello, D. Berg-Lyons, A. Gonzalez, J. Stombaugh, D. Knights, P. Gajer, J. Ravel, N. Fierer *et al.*, Moving pictures of the human microbiome, Genome Biol. **12**, R50 (2011).

[4] H. Beaumont, J. Gallie, C. Kost, G. Ferguson, and P. Rainey, Experimental evolution of bet hedging, Nature (London) **462**, 90 (2009).

[5] P. Visco, R. J. Allen, S. N. Majumdar, and M. R. Evans, Switching and growth for microbial populations in catastrophic responsive environments, Biophys. J. **98**, 1099 (2010).

[6] R. M. May, *Stability and Complexity in Model Ecosystems* (Princeton University Press, Princeton, NJ, 1973).

[7] S. Karlin and B. Levikson, Temporal fluctuations in selection intensities: Case of small population size, Theor. Popul. Biol. **6**, 383 (1974).

[8] P. L. Chesson and R. R. Warner, Environmental variability promotes coexistence in lottery competitive systems, Am. Nat. **117**, 923 (1981).

[9] M. Loreau and C. de Mazancourt, Species synchrony and its drivers: Neutral and nonneutral community dynamics in fluctu-ating environments, Am. Nat. **172**, E48 (2008).

[10] B. K. Xue and S. Leibler, Bet Hedging against Demographic Fluctuations, Phys. Rev. Lett. **119**, 108103 (2017).

[11] M. Thattai and A. Van Oudenaarden, Stochastic gene expres-sion in fluctuating environments, Genetics **167**, 523 (2004).

[12] E. Kussell and S. Leibler, Phenotypic diversity, population growth, and information in fluctuating environments, Science **309**, 2075 (2005).

[13] M. Assaf, A. Kamenev, and B. Meerson, Population extinction in a time-modulated environment, Phys. Rev. E **78**, 041123 (2008).

[14] M. Assaf, A. Kamenev, and B. Meerson, Population extinction risk in the aftermath of a catastrophic event, Phys. Rev. E **79**, 011127 (2009).

[15] R. A. Chisholm, R. Condit, K. A. Rahman, P. J. Baker, S. Bunyavejchewin, Y. Chen, G. Chuyong, H. S. Dattaraja, S. Davies, C. E. N. Ewango *et al.*, Temporal variability of forest communities: empirical estimates of population change in 4000 tree species, Ecol. Lett. **17**, 855 (2014).

[16] D. A. Kessler and N. Shnerb, Neutral-like abundance distri-butions in the presence of selection in a continuous fitness landscape, J. Theor. Biol. **345**, 1 (2014).

[17] M. Kalyuzhny, R. Kadmon, and N. M. Shnerb, A neutral theory with environmental stochasticity explains static and dy-namic properties of ecological communities, Ecol. Lett. **18**, 572 (2015).

[18] M. Assaf, E. Roberts, Z. Luthey-Schulten, and N. Goldenfeld, Extrinsic Noise Driven Phenotype Switching in a Self-Regulating Gene, Phys. Rev. Lett. **111**, 058102 (2013).

[19] Q. He, M. Mobilia, and U. C. Täuber, Spatial rock-paper-scissors models with inhomogeneous reaction rates, Phys. Rev. E **82**, 051909 (2010).

[20] U. Dobramysl and U. C. Täuber, Environmental Versus Demo-graphic Variability in Two-Species Predator-Prey Models, Phys. Rev. Lett. **110**, 048105 (2013).

[21] M. Assaf, M. Mobilia, and E. Roberts, Cooperation Dilemma in Finite Populations under Fluctuating Environments, Phys. Rev. Lett. **111**, 238101 (2013).

[22] E. Roberts, S. Be'er, C. Bohrer, R. Sharma, and M. Assaf, Dynamics of simple gene-network motifs subject to extrinsic fluctuations, Phys. Rev. E **92**, 062717 (2015).

[23] A. Melbinger and M. Vergassola, The impact of environmen-tal fluctuations on evolutionary fitness functions, Sci. Rep. **5**, 15211 (2015).

[24] M. Assaf and B. Meerson, WKB theory of large deviations in stochastic populations, J. Phys. A: Math. Theor. **50**, 263001 (2017).

[25] O. Vilk and M. Assaf, Population extinction under bursty re-production in a time-modulated environment, Phys. Rev. E **97**, 062114 (2018).

[26] U. Dobramysl, M. Mobilia, M. Pleimling, and U. C. Täuber, Stochastic population dynamics in spatially extended predator-prey systems, J. Phys. A: Math. Theor. **51**, 063001 (2018).

[27] L. Marrec and A.-F. Bitbol, Resist or perish: Fate of a microbial population subjected to a periodic presence of antimicrobial, PLoS Comput. Biol. **16**, e1007798 (2020).

[28] J. F. Crow and M. Kimura, *An Introduction to Population Ge-netics Theory* (Blackburn Press, Caldwell, NJ, 2009).

[29] W. J. Ewens, *Mathematical Population Genetics* (Springer, New York, 2004).

[30] R. A. Blythe and A. J. McKane, Stochastic models of evolu-tion in genetics, ecology and linguistics, J. Stat. Mech. (2007) P07018.

[31] R. M. Nowak, *Evolutionary Dynamics* (Belknap Press, Cam-bridge, MA, 2006).

[32] K. Wienand, E. Frey, and M. Mobilia, Evolution of a Fluctu-ating Population in a Randomly Switching Environment, Phys. Rev. Lett. **119**, 158301 (2017).

[33] K. Wienand, E. Frey, and M. Mobilia, Eco-evolutionary dynam-ics of a population with randomly switching carrying capacity, J. R. Soc., Interface **15**, 20180343 (2018).

[34] J. Roughgarden, *Theory of Population Genetics and Evolution-ary Ecology: An Introduction* (Macmillan, New York, 1979).

[35] A. Melbinger, J. Cremer, and E. Frey, Evolutionary Game Theory in Growing Populations, Phys. Rev. Lett. **105**, 178101 (2010).

[36] J. Cremer, A. Melbinger, and E. Frey, Evolutionary and population dynamics: A coupled approach, Phys. Rev. E **84**, 051921 (2011).

[37] J. Cremer, A. Melbinger, and E. Frey, Growth dynamics and the evolution of cooperation in microbial populations, Sci. Rep. **2**, 281 (2012).

[38] A. Melbinger, J. Cremer, and E. Frey, The emergence of cooperation from a single mutant during microbial life cycles, J. R. Soc., Interface **12**, 20150171 (2015).

[39] C. S. Gokhale and C. Hauert, Eco-evolutionary dynamics of social dilemmas, Theor. Popul. Biol. **111**, 28 (2016).

[40] J. S. Chuang, O. Rivoire, and S. Leibler, Simpson's paradox in a synthetic microbial system, Science **323**, 272 (2009).

[41] L. M. Wahl, P. J. Gerrish, and I. Saika-Voivod, Evaluating the impact of population bottlenecks in experimental evolution, Genetics **162**, 961 (2002).

[42] K. Wienand, M. Lechner, F. Becker, H. Jung, and E. Frey, Non-selective evolution of growing populations, PLoS One **10**, e0134300 (2015).

[43] J. Coates, B. R. Park, D. Le, E. Şimşek, W. Chaudhry, and M. Kim, Antibiotic-induced population fluctuations and stochastic clearance of bacteria, eLife **7**, e32976 (2018).

[44] Z. Patwa and L. M. Wahl, Adaptation rates of lytic viruses depend critically on whether host cells survive the bottleneck, Evolution **64**, 1166 (2009).

[45] P. B. Rainey and K. Rainey, Evolution of cooperation and conflict in experimental bacterial populations, Nature (London) **425**, 72 (2003).

[46] M. A. Brockhurst, A. Buckling, and A. Gardner, Cooperation peaks at intermediate disturbance, Curr. Biol. **17**, 761 (2007).

[47] M. A. Brockhurst, Population bottlenecks promote cooperation in bacterial biofilms, PLoS One **2**, e634 (2007).

[48] J. Cremer, A. Melbinger, K. Wienand, T. Henriquez, H. Jung, and E. Frey, Cooperation in microbial populations: Theory and experimental model systems, J. Mol. Biol. **431**, 4599 (2019).

[49] A. Kamenev, B. Meerson, and B. Shklovskii, How Colored Environmental Noise Affects Population Extinction, Phys. Rev. Lett. **101**, 268103 (2008).

[50] B. Gaál, J. W. Pitchford, and A. J. Wood, Exact results for the evolution of stochastic switching in variable asymmetric environments, Genetics **184**, 1113 (2010).

[51] P. Ashcroft, P. M. Altrock, and T. Galla, Fixation in finite populations evolving in fluctuating environments, J. R. Soc., Interface **11**, 20140663 (2014).

[52] M. Danino and N. M. Shnerb, Fixation and absorption in a fluctuating environment, J. Theor. Biol. **441**, 84 (2018).

[53] P. G. Hufton, Y. T. Lin, and T. Galla, Phenotypic switching of populations of cells in a stochastic environment, J. Stat. Mech.: Theory Exp. (2018) 023501.

[54] P. G. Hufton, Y. T. Lin, T. Galla, and A. J. McKane, Intrinsic noise in systems with switching environments, Phys. Rev. E **93**, 052119 (2016).

[55] R. West, M. Mobilia, and A. M. Rucklidge, Survival behavior in the cyclic Lotka-Volterra model with a randomly switching reaction rate, Phys. Rev. E **97**, 022406 (2018).

[56] E. Kussell, R. Kishony, N. Q. Balaban, and S. Leibler, Bacterial persistence: A model of survival in changing environments, Genetics **169**, 1807 (2005).

[57] M. Acar, J. Mettetal, and A. van Oudenaarden, Stochastic switching as a survival strategy in fluctuating environments, Nat. Genet. **40**, 471 (2008).

[58] N. Q. Balaban, J. Merrin, R. Chait, L. Kowalik, and S. Leibler, Bacterial persistence as a phenotypic switch, Science **305**, 1622 (2004).

[59] A. Taitelbaum, R. West, M. Assaf, and M. Mobilia, Population Dynamics in a Changing Environment: Random versus Periodic Switching, Phys. Rev. Lett. **125**, 048105 (2020).

[60] S. Shibasaki, M. Mobilia, and S. Mitri, Exclusion of the fittest predicts microbial community diversity in fluctuating environments, J. R. Soc., Interface **18**, 20210613 (2021).

[61] R. West and M. Mobilia, Fixation properties of rock-paper-scissors games in fluctuating populations, J. Theor. Biol. **491**, 110135 (2020).

[62] R. Cavicchioli, W. J. Ripple, K. N. Timmis, F. Azam, L. R. Bakken, M. Baylis, M. J. Behrenfeld, A. Boetius, P. W. Boyd, A. T. Classen *et al.*, Scientists warning to humanity: microorganisms and climate change, Nat. Rev. Microbiol. **17**, 569 (2019).

[63] J. Nguyen, J. Lara-Gutiérrez, and R. Stocker, Environmental fluctuations and their effects on microbial communities, populations and individuals, FEMS Microbiol. Rev. **45**, fuaa068 (2021).

[64] J. R. Bernhardt, J. M. Sunday, and M. I. O'Connor, Metabolic theory and the temperature-size rule explain the temperature dependence of population carrying capacity, Am. Nat. **192**, 687 (2018).

[65] V. M. Savage, J. E. Gillooly, J. H. Brown, G. B. West, and E. L. Charnov, Effects of body size and temperature on population growth, Am. Nat. **163**, 429 (2004).

[66] B. Descamps-Julien and A. Gonzalez, Stable coexistence in a fluctuating environment: an experimental demonstration, Ecology **86**, 2815 (2005).

[67] See Supplemental Material at http://link.aps.org/supplemental/10.1103/PhysRevResearch.5.L022004 for details about the EN statistics, simulations, the PSD, mean fixation time, and the case of a public good scenario, which includes Refs. [22,76–79], and is also available alongside simulation source codes and data in Ref. [75].

[68] C. W. Gardiner, *Handbook of Stochastic Methods* (Springer, New York, 2002).

[69] W. Horsthemke and R. Lefever, *Noise-Induced Transitions* (Springer, Berlin, 2006).

[70] I. Bena, Dichotomous noise: exact results for out-of-equilibrium systems, Int. J. Mod. Phys. B **20**, 2825 (2006).

[71] There is a third timescale, which is exponential in $K_0 \gg 1$, and corresponds to the extinction of the entire population. Notably, in Sec. A5 of SM [67] we consider a public good scenario involving only the last two timescales.

[72] T. Antal and I. Scheuring, Fixation of strategies for an evolutionary game in finite populations, Bull. Math. Biol. **68**, 1923 (2006).

[73] M. H. A. Davis, Piecewise-deterministic Markov processes: A general class of non-diffusion stochastic models, J. R. Stat. Soc., B: Stat. Methodol. **46**, 353 (1984).

[74] F. Abdul-Rahman, D. Tranchina, and D. Gresham, Fluctuating environments maintain genetic diversity through neutral fitness effects and balancing selection, Mol. Biol. Evol. **38**, msab173 (2021).

[75] https://doi.org/10.6084/m9.figshare.21603480.v1

[76] D. T. Gillespie, A general method for numerically simulating the stochastic time evolution of coupled chemical reactions, J. Comput. Phys. **22**, 403 (1976).

[77] D. F. Anderson, A modified next reaction method for simulating chemical systems with time dependent propensities and delays, J. Chem. Phys. **127**, 214107 (2007).

[78] D. T. Gillespie, Approximate accelerated stochastic simulation of chemically reacting systems, J. Chem. Phys. **115**, 1716 (2001).

[79] E. Berríos-Caro and T. Galla, Beyond the adiabatic limit in systems with fast environments: A τ-leaping algorithm, Phys. Rev. E **104**, 014122 (2021).